Egyptian Journal of Radiology and Nuclear Medicine

RESEARCH Open Access

Evaluation of liver parenchymal changes in patients with reduced left ventricular ejection fraction using cardiac MRI T1 mapping and extracellular volume fraction

Sercan Şahin[1*], Hazal Öykü Yılmaz[2], Can Ilgın[3] and Nilgün Işıksalan Özbülbül[2]

Abstract

Background and objectives Congestive hepatopathy (CH) is a diffuse parenchymal liver disease resulting from chronic passive congestion due to cardiac pathology. This retrospective cross-sectional study aims to evaluate hepatic congestion in patients with left ventricular ejection fraction (LVEF) <50% using cardiac magnetic resonance imaging (CMR) T1 mapping and extracellular volume (ECV) fraction.

Methods We analyzed 103 patients with LVEF <50% and 80 controls with normal CMR findings and no prior disease. Regions of interest in the liver parenchyma, interventricular myocardium, and left ventricular blood pool were placed on pre- and post-contrast T1 maps to calculate ECV. Receiver operating characteristic (ROC) analysis assessed the area under the curve (AUC) and optimal cutoff values for predicting reduced LVEF. Spearman's correlation evaluated associations between T1/ECV values, left ventricular parameters, and biochemical tests.

Results Liver pre-contrast T1 (p<0.001), post-contrast T1 (p=0.032), and ECV (p<0.001) were significantly higher in patients than in controls. Myocardial native T1 (p<0.001) and ECV (p<0.001) were elevated, whereas post-contrast T1 was lower (p=0.012). Liver pre-contrast T1 yielded the highest AUC (0.949) with a cutoff of 608.16 ms (sensitivity 88.3%, specificity 95.0%), outperforming all myocardial and other liver parameters. Native liver T1 correlated with stroke volume index (ρ=−0.461), left ventricular end-diastolic (ρ=0.301) and end-systolic indexes (ρ=0.572), NT-proBNP (ρ=0.324), and GGT (ρ=0.360) (all p<0.001).

Conclusions Routine CMR pre-contrast liver T1 mapping facilitates early detection and quantification of CH in patients with reduced LVEF, potentially preceding overt clinical or laboratory abnormalities.

Keywords Magnetic resonance imaging, Heart failure, Liver congestion

Introduction

Congestive hepatopathy (CH) is a hepatic parenchymal disease resulting from passive and chronic congestion secondary to elevated central venous pressure (CVP), primarily stemming from underlying cardiac pathology or dysfunction [1]. Advances in medical and interventional therapies have significantly increased the life expectancy of heart failure (HF) patients, leading to more frequent encounters with CH by clinicians and radiologists [2]. Studies have reported that the

*Correspondence:
Sercan Şahin
sercansahinmd@gmail.com
[1] Radiology Department, Ayvalık State Hospital, Balıkesir, Turkey
[2] Radiology Department, Ankara Bilkent City Hospital, Ankara, Turkey
[3] Radiation Oncology Department, Istanbul Faculty of Medicine, Istanbul University, Istanbul, Turkey

© The Author(s) 2026. **Open Access** This article is licensed under a Creative Commons Attribution 4.0 International License, which permits use, sharing, adaptation, distribution and reproduction in any medium or format, as long as you give appropriate credit to the original author(s) and the source, provide a link to the Creative Commons licence, and indicate if changes were made. The images or other third party material in this article are included in the article's Creative Commons licence, unless indicated otherwise in a credit line to the material. If material is not included in the article's Creative Commons licence and your intended use is not permitted by statutory regulation or exceeds the permitted use, you will need to obtain permission directly from the copyright holder. To view a copy of this licence, visit http://creativecommons.org/licenses/by/4.0/.

prevalence of CH in this patient population ranges widely, from 15 to 80%, depending on the severity of HF [3, 4]. If not addressed promptly, hepatic congestion may progress to impaired liver function, parenchymal fibrosis, cirrhosis, and even hepatocellular carcinoma [5].

T1 and T2 mapping techniques, along with extracellular volume (ECV) calculation, enable quantitative assessment of myocardial tissue characteristics when integrated into conventional cardiac magnetic resonance imaging (CMR) protocols and have become indispensable components of cardiac imaging in recent years [6]. In T1 mapping, images are typically acquired in the short-axis and two-chamber planes, often including portions of the liver. Previous studies have reported prolonged T1 and increased ECV values in the liver parenchyma of patients with various cardiovascular conditions; such as dilated cardiomyopathy [7, 8], repaired tetralogy of Fallot and Fontan circulation [9], HF, atrial fibrillation, and coronary artery disease [10] when compared to healthy controls. Therefore, this study evaluates the liver parenchymal changes in patients with a left ventricular ejection fraction (LVEF) below 50%, irrespective of specific underlying cardiac diagnoses, using T1 mapping sequences and ECV measurements on CMR.

Methods

Study population

This retrospective study included patients who underwent CMR between April 2023 and December 2023 at the Ankara Bilkent City Hospital. Demographic, clinical, and laboratory data were obtained from the hospital information system. Participants were categorized into two groups: those with an LVEF below 50% as assessed on cine images and those who underwent CMR for various indications without pathology identified on imaging and no known prior disease. Patients were excluded from the study if adequate image quality was not achieved, mapping sequences were not performed, or demographic, clinical, and laboratory data were unavailable. Additionally, patients with known conditions affecting the liver parenchyma were also excluded. Following these criteria, 195 patients were evaluated. After excluding 3 patients whose livers were not included in the imaging, 2 patients with human immunodeficiency virus infection receiving systemic antiviral therapy, 2 patients undergoing chemotherapy, 2 patients with missing demographic and laboratory data, 1 patient on medication for hyperlipidemia, 1 patient receiving systemic treatment for systemic lupus erythematosus, and 1 patient diagnosed with hereditary fructose intolerance, the final study population consisted of 183 patients.

CMR imaging protocols

Imaging was performed using a 1.5 Tesla MRI system (General Electric Signa™ Explorer, Milwaukee, WI, USA) equipped with phased-array surface body coils, located in the Radiology Clinic of the Ankara Bilkent City Hospital. All acquisitions were synchronized with the cardiac cycle using vector cardiographic gating.

LVEF was calculated from short-axis and two-chamber cine images, acquired using balanced steady-state free precession gradient echo sequences with retrospective electrocardiography gating throughout the cardiac cycle. The sequence parameters are summarized in Supplementary Table 1.

Both native and post-contrast T1 mapping images were acquired in the short-axis plane at the mid-ventricular level using the Modified Look-Locker Inversion Recovery (MOLLI) 3(3)3(3)5 sequence. Detailed sequence parameters are provided in Supplementary Table 2. Post-contrast images were obtained approximately 10 min after the intravenous administration of a 7.5 mL bolus of gadobutrol-containing contrast agent (Gadovist®, 1 mmol/mL; Bayer AG, Germany).

Assessment of CMR images and quantitative measurements

CMR images were retrospectively retrieved from our hospital's Picture Archiving and Communication System. Image evaluations were cınducted by a fifth-year radiology resident and a radiology specialist with approximately 15 years of experience in CMR, using the departmental workstations (Advantage Workstation VolumeShare 7, GE Healthcare, Wisconsin, USA). To assess intra-observer agreement, the fifth-year resident repeated the measurements three months after the initial assessment. For inter-observer agreement, measurements from a third-year radiology resident were compared with those of the primary observer in a randomly selected subset of 50 participants.

Stroke volume, LVEF, and left ventricular end-diastolic (LVED) and end-systolic (LVES) volumes were calculated from short-axis cine images using a semi-automated method with the "Cardiac VX" software on dedicated workstations. Using the same workstations and the "READY View" software, measurements were acquired from native and post-contrast T1 mapping images acquired at mid-ventricular short-axis levels by drawing appropriate regions of interest (ROI). In both native and post-contrast T1 maps, measurements were obtained at three separate locations within the liver parenchyma, carefully avoiding vascular structures and bile ducts. Round ROIs were drawn, and the arithmetic mean of the three measurements was recorded. Additionally, T1

values were measured by manually placing ROIs within the interventricular septal myocardium and the left ventricular blood pool, using round ROIs (Fig. 1). All values were recorded in milliseconds (ms).

Statistical analysis

Statistical analyses were performed using IBM SPSS Statistics for Windows, Version 25.0 (IBM Corp., Armonk, NY, USA). The Kolmogorov–Smirnov and Shapiro–Wilk tests, along with histogram analyses, were used to assess the normality of continuous variables. Normally distributed continuous variables were presented as mean ± standard deviation, while non-normally distributed variables were expressed as median and interquartile range (Q1–Q3). Categorical variables were summarized as counts and percentages.

For statistical comparisons, the chi-square test was used for categorical variables. Comparisons of continuous variables between two independent groups were performed using either the Student's *t*-test (for normally distributed data) or the Mann–Whitney *U* test (for non-normally distributed data).

Receiver operating characteristic (ROC) curve analysis and area under the curve (AUC) values were used to evaluate the diagnostic performance (sensitivity and specificity) of continuous variables. The Pearson correlation test was used to assess relationships between normally distributed continuous variables, while the Spearman correlation test was used for non-normally distributed variables. Correlation coefficients were interpreted as follows: 0.00–0.19 = none or very weak, 0.20–0.39 = weak, 0.40–0.59 = moderate, 0.60–0.79 = strong, and 0.80–1.00 = very strong.

Intraobserver and interobserver agreement were assessed using intraclass correlation coefficients (ICC) and the coefficient of variation (CV). ICC values <0.50 were considered poor, 0.50–0.75 moderate, 0.75–0.90 good, and >0.90 excellent. CV values <10% were considered good, 10–20% acceptable, and >20% above the acceptable threshold. A *p*-value <0.05 was considered statistically significant.

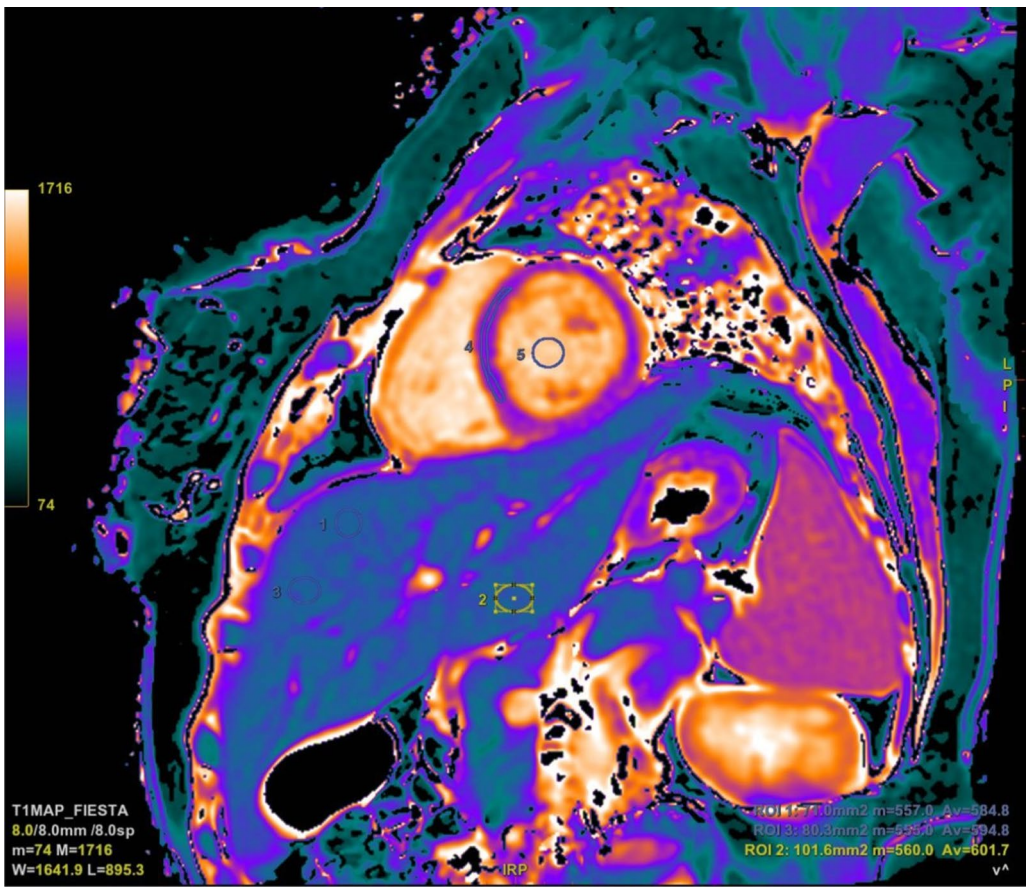

Fig. 1 Native T1 mapping image. Region of interest placement for T1 relaxation time measurements in the liver parenchyma, interventricular myocardium, and left ventricular blood pool on native T1 mapping images

Results

In this study, 80 participants without detectable pathology and no prior disease served as the control group, while 103 patients with an LVEF below 50% constituted the pathological group.

T1 mapping results

In native T1 mapping, the median T1 values in the liver parenchyma and interventricular myocardium of the control group were 568.66 ms (538.08–589.58) and 953.50 ms (930.25–986.75), respectively. In the patient group, T1 values measured from the same locations were significantly higher: 646.33 ms (625.33–688.33) for the liver and 1028 ms (994–1071) for the myocardium, with a significant difference noted for both ($p < 0.001$) (Table 1).

Post-contrast T1 mapping and ECV measurements results

Post-contrast T1 mapping revealed the median T1 value of the liver parenchyma was 324.33 ms (305.33–379.33) in the control group, compared to 343 ms (311–403.82) in the patient group, indicating a significant difference ($p = 0.032$). For the interventricular myocardium, post-contrast T1 values were 475 ms (420–558) in controls versus 435 ms (365.5–532.5) in patients, also significant ($p = 0.012$) (Table 2).

ECV values were calculated using pre- and post-contrast T1 measurements along with hematocrit levels. The liver parenchymal ECV was 33.8% (28.6–36.8) in the control group and 37.8% (34.7–49.7) in the patient group, reflecting a statistically significant difference ($p < 0.001$). The ECV of the interventricular myocardium was 26.3% (22.7–30) in the control group and 36.6% (30.2–52.8) in the patient group, also demonstrating a statistically significant difference ($p < 0.001$).

Table 1 Comparison of native T1 mapping measurements from the liver parenchyma and interventricular septum between control and patient groups

	Control group (n=80)	Patient group (n=103)	*p* value
Liver parenchyma (ms)	568.66(538.08 – 589.58)	646.33(625.33 – 688.33)	<0.001
Interventricular myocardium (ms)	953.50(930.25 – 986.75)	1028(994 – 1071)	<0.001

ROC curve analysis

ROC curve analysis of native T1 mapping values from the liver parenchyma and interventricular myocardium yielded AUCs of 0.949 (95% CI: 0.918–0.981) and 0.873 (95% CI: 0.823–0.922), respectively. Both parameters demonstrated statistically significant diagnostic performance ($p < 0.001$ for both) (Fig. 2A). In contrast, ROC analysis of post-contrast T1 values showed an AUC of 0.593 for the liver and 0.609 for the myocardium. However, the AUCs for the corresponding ECV values improved, at 0.725 for the liver and 0.793 for the myocardium, suggesting better diagnostic performance (Fig. 2B).

In native T1 mapping, a cut-off value of 608.166 ms for the liver parenchyma was identified using the Youden index on the ROC curve. At this threshold, the sensitivity and specificity were 88.3% and 95%, respectively. Participants were divided based on this cut-off: In the first group (n = 86), with liver parenchyma native T1 values < 608.166 ms, the mean left ventricular stroke volume was 71.64 ± 14.78 mL. In the second group (n = 91), with T1 values ≥ 608.166 ms, the mean stroke volume was 57.15 ± 21.73 mL. This difference between the two groups was statistically significant ($p < 0.001$). The stroke volume index, calculated by dividing the left ventricular stroke volume by the body surface area (determined using the Du Bois formula), was 39.74 ± 9.49 mL/m^2 in the first group and 30.59 ± 11.19 mL/m^2 in the second group. This difference was statistically significant ($p < 0.001$). LVED volumes were measured as 122.41 ± 27.22 mL in the first group and 162.70 ± 60.08 mL in the second group, with the difference between the groups reaching statistical significance ($p < 0.001$). LVED volume indices were calculated as 66.66 ± 14.23 mL/m^2 in the first group and 86.31 ± 28.12 mL/m^2 in the second group, with a statistically significant difference between the two groups ($p < 0.001$). LVES volume was 46.5 (37.75–58) mL in the first group and 93 (63–131) mL in the second group, demonstrating a statistically significant difference ($p <$

Table 2 Post-contrast T1 and extracellular volume values

	Control group (n=79)	Patient group (n=101)	*p* value
Liver parenchyma (ms)	324.33(305.33 – 379.33)	343(311 – 403.82)	0.032
Interventricular myocardium (ms)	475(420 – 558)	435(365.5 – 532.5)	0.012
Liver parenchyma ECV (%)	33.8(28.6 – 36.8)	37.8(34.7 – 49.7)	<0.001
Myocardium ECV (%)	26.3(22.7 – 30)	36.6(30.2 – 52.8)	<0.001

ECV = extracellular volume

0.001). Similarly, the LVES volume index was calculated as 25.17 (19.59–29.91) mL/m^2 in the first group and 49.82 (33.21–67.63) mL/m^2 in the second group, also showing a statistically significant difference between the two groups ($p < 0.001$) (Table 3).

Correlations with laboratory parameters

The correlations between native liver parenchymal T1 and ECV values and laboratory parameters—including NT-proBNP (N-terminal pro b-type natriuretic peptide), AST (aspartate aminotransferase), ALT (alanine aminotransferase), GGT (gamma-glutamyl transferase), and ALP (alkaline phosphatase) levels—in patients with a LVEF below 50% are summarized in Table 4. Native liver T1 values correlated weakly with NT-proBNP (ρ = 0.324, p = 0,001) and GGT levels (ρ = 0.360, $p < 0.001$). However, liver parenchymal ECV values did not show

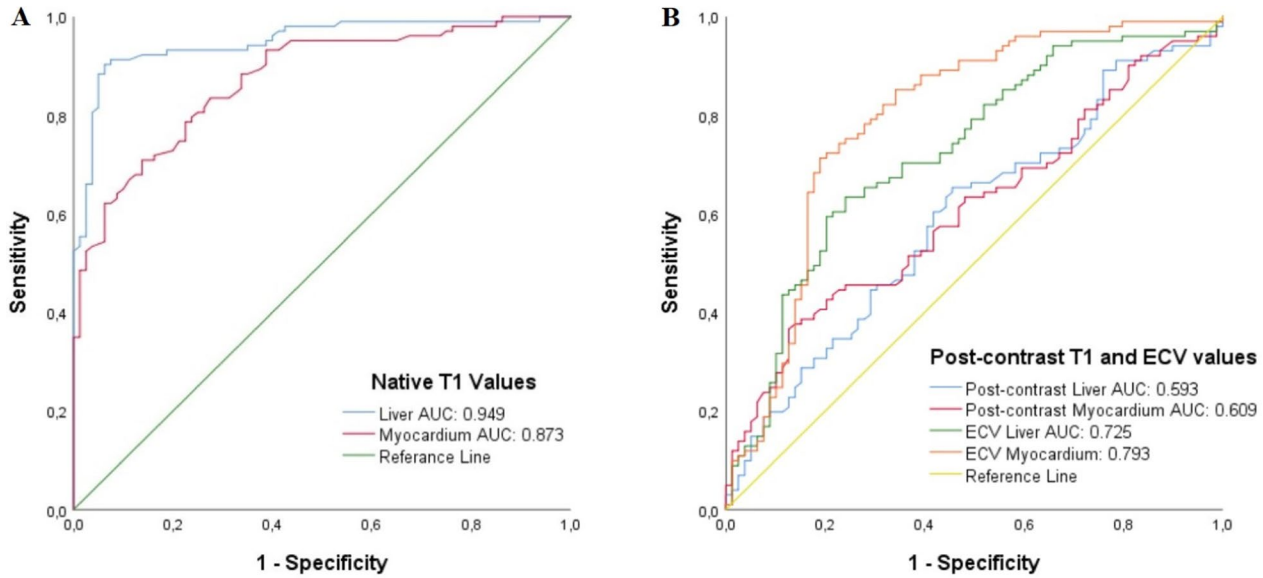

Fig. 2 ROC curves of native and post-contrast T1 values and ECV measurements of the liver and myocardium for differentiating between control and patient groups. AUC = area under the curve; ECV = extracellular volume; ROC = receiver operating characteristic

Table 3 Cardiac hemodynamic parameters stratified by the 608.166 ms cut-off in liver native T1 mapping

	Liver native T1 <608.166 ms (n=86)	Liver native T1 ≥ 608.166 ms (n=91)	*p* value
Stroke volume (mL)	71.64±14.78	57.15±21.73	<0.001
Stroke volume index (mL/m^2)	39±7.49	30.59±11.19	<0.001
LVED volume (mL)	122.41±27.22	162.7±60.08	<0.001
LVED volume index (mL/m^2)	66.66±14.23	86.31±28.12	<0.001
LVES volume index (mL)	46.5(37.75 – 58)	93(63 – 131)	<0.001
LVES volume index (mL/m^2)	25.17(19.59 – 29.91)	49.82(33.21 – 67.63)	<0.001

LVED = left ventricular end-diastolic; LVES = left ventricular end-systolic

Table 4 Correlation of liver native T1 and ECV values with biochemical parameters

	NT-proBNP	ALT	AST	GGT	ALP
Liver native T1 (ms)	$\rho = 0.324$ $p = 0.001$	$\rho = 0.190$ $p = 0.054$	$\rho = 0.191$ $p = 0.053$	$\rho = 0.360$ $p < 0.001$	$\rho = 0.165$ $p = 0.960$
Liver ECV (%)	$\rho = 0.031$ $p = 0.759$	$\rho = -0.150$ $p = 0.135$	$\rho = -0.028$ $p = 0.783$	$\rho = 0.024$ $p = 0.810$	$\rho = 0.180$ $p = 0.072$

ρ = Spearman's correlation coefficient; ALP = alkaline phosphatase; ALT = alanine aminotransferase; AST = aspartate aminotransferase; ECV = extracellular volume; GGT = gamma-glutamyl transferase; NT-proBNP = N-terminal pro–B-type natriuretic peptide

a statistically significant correlation with any of the assessed blood parameters.

Correlations between liver and myocardium values

The correlations between the native T1 and ECV values of the liver parenchyma and those of the interventricular myocardium are summarized in Table 5. Native liver T1 values exhibited a moderate correlation with myocardial native T1 values ($\rho = 0.563$; $p < 0.001$), and weak correlations with both liver ECV values ($\rho = 0.311$; $p < 0.001$) and myocardial ECV values ($\rho = 0.379$; $p < 0.001$). Liver parenchymal ECV values demonstrated a moderate correlation with myocardial ECV values ($\rho = 0.568$; $p < 0.001$), and weak correlations with both native liver T1 values ($\rho = 0.311$; $p < 0.001$) and myocardial native T1 values ($\rho = 0.338$; $p < 0.001$).

Intra- and inter-observer agreement

Intra-observer agreement was evaluated by repeating the native and post-contrast liver parenchymal measurements in 50 randomly selected participants, three months after the initial evaluation, by a fifth-year radiology resident. The ICC for native liver T1 values was 0.989 (95% Confidence Interval: 0.980–0.993), with a CV of 1.3%, indicating excellent intra-observer consistency. For liver ECV values, the ICC was 0.941 (95% CI: 0.895–0.967), with a CV of 5.5%, reflecting good to excellent intra-observer consistency.

Inter-observer agreement was assessed by a third-year radiology resident independently repeated the native and post-contrast T1 measurements in the same group of 50 participants. The ICC for native liver T1 values was 0.927 (95% CI: 0.871–0.959), with a CV of 3.2%, indicating good to excellent inter-observer consistency. For liver ECV values, the ICC was 0.920 (95% CI: 0.855–0.955), and the CV was 7.5%, also indicating good to excellent inter-observer agreement (Table 6).

Discussion

Heart failure is a complex clinical syndrome characterized by signs and symptoms that occur at rest or during physical activity, resulting from elevated intracardiac pressure, reduced ventricular ejection, or a combination of both, due to underlying structural or functional abnormalities [11]. Advances in medical and interventional treatments have prolonged the life expectancy of patients with heart failure, and the growing elderly population is contributing to a global increase in the prevalence of this condition [12]. CH is a parenchymal liver disease resulting from chronic passive hepatic congestion, typically caused by elevated CVP secondary to cardiac dysfunction [1]. With the rising prevalence of HF and improved survival among affected patients, CH is increasingly encountered by clinicians and radiologists in practice [2].

CMR is considered an advanced imaging modality, facilitating comprehensive anatomical and functional evaluation of the heart, as well as tissue characterization through contrast-enhanced sequences and mapping techniques [13]. Recent studies have demonstrated that various measurements obtained from the liver parenchyma, which is often included in CMR mapping sequences, enable the quantitative evaluation of structural changes within the liver [7–10]. T1 relaxation times correlate with histological changes in chronic liver disease, liver stiffness measurements obtained using FibroScan, and clinical severity scores such as

Table 5 Correlation between liver native T1 and ECV values and the corresponding native T1 and ECV values of the interventricular myocardium

	Liver native T1	Liver ECV	Myocardium native T1	Myocardium ECV
Liver native T1 (ms)	$\rho = 1.000$ –	$\rho = 0.311$ $p < 0.001$	$\rho = 0.563$ $p < 0.001$	$\rho = 0.379$ $p < 0.001$
Liver ECV (%)	$\rho = 0.311$ $p < 0.001$	$\rho = 1.000$ –	$\rho = 0.338$ $p < 0.001$	$\rho = 0.568$ $p < 0.001$

ρ = Spearman's correlation coefficient; ECV = extracellular volume.

Table 6 Intraclass correlation coefficients and coefficient of variation for intra-observer and inter-observer measurements

	Intra-observer			Inter-observer		
	ICC	%95 CI	CV(%)	ICC	%95 CI	CV(%)
Liver native T1	0.989	0.980 – 0.993	1.3	0.927	0.871 – 0.959	3.2
Liver ECV	0.941	0.895 – 0.967	5.5	0.920	0.855 – 0.955	7.5

CI = confidence interval; CV = coefficient of variation; ECV =, extracellular volume; ICC = intraclass correlation coefficient

the Child–Pugh score and the Model for End-Stage Liver Disease [14, 15]. These findings support the use of T1 mapping as a valuable tool for assessing liver parenchymal changes.

In our study, the native liver parenchymal T1 values in the patient group were 646.33 ms, compared to 568.66 ms in the control group, and the difference was statistically significant. Similarly, patients with idiopathic dilated cardiomyopathy were compared to a control group and reported liver parenchymal T1 values significantly higher in the patient group [8], consistent with our findings. In a retrospective study conducted in the pediatric population, was demonstrated that native liver T1 values in the control group were significantly lower than those in patients with bidirectional cavopulmonary anastomosis and Fontan circulation [16]. When these studies—based on different etiologies and including control groups—are considered alongside our findings, it can be inferred that various pathologies leading to elevated CVP due to cardiac dysfunction result in hepatic congestion, interstitial fibrosis, and an associated increase in T1 values on parametric maps.

Myocardial native T1 values in the patient group were recorded as 1028 ms, compared to 953.50 ms in the control group, and the difference was statistically significant. ROC analysis revealed an AUC of 0.949 for liver parenchymal T1 values and 0.873 for myocardial T1 values, indicating that liver parenchymal T1 measurements are more effective in distinguishing between the patient and control groups than myocardial T1 measurements. In the same study, Huber et al. [8] divided the patient group into two subgroups: those with stable dilated cardiomyopathy without clinical signs of HF, and those with unstable dilated cardiomyopathy exhibiting congestive HF. They demonstrated that native liver T1 values could differentiate between these two subgroups with high sensitivity (100%) and specificity (79%) at a cutoff value of 585 ms. While myocardial T1 values did not differ significantly between the subgroups, LVEF and CMR strain parameters contributed to the distinction, albeit with lower sensitivity and specificity compared to native liver T1 values.

In native T1 mapping, a cutoff value of 608.17 ms for the liver parenchyma was determined using the Youden method, yielding a sensitivity of 88.3% and a specificity of 95%. In the study by Bogaert et al. [17], conducted using an MRI scanner from a different manufacturer with a 1.5 T magnetic field strength (Ingenia, Philips Healthcare, The Netherlands), the cutoff value for native liver parenchymal T1 was identified as 617 ms, with a sensitivity of 79.5% and a specificity of 91%. These values are notably similar to those observed in our study.

In our study, participants with liver parenchymal native T1 values below 608.166 ms had significantly higher left ventricular stroke volume and stroke index compared to those with T1 values. In this group, LVED volume and index, as well as LVES volume and index, were significantly lower than in the latter group. These findings suggest that native T1 values of the liver parenchyma may serve as predictive markers for hemodynamic alterations. Prolongation of T1 relaxation times is likely associated with elevated CVP and congestion in the liver parenchyma. We propose that native liver T1 mapping could be useful not only for prediction but also for guiding the clinical management of these hemodynamic disturbances.

Furthermore, post-contrast images revealed significantly elevated T1 and ECV values in the liver parenchyma of the patient group compared to controls. The ROC analysis indicated that ECV is more effective than post-contrast T1 in distinguishing between the two groups. This aligns with findings from Kazour et al. [9], who reported similar AUC values for ECV relative to post-contrast T1, suggesting that ECV may provide additional insights in assessing liver conditions in cardiac patients.

Importantly, we observed a moderate correlation between liver parenchymal native T1 values and interventricular myocardial native T1 values ($\rho = 0.563$). A similar correlation was reported by Beigh et al. [18] in their retrospective study of patients with a functional single ventricle, where they found a correlation coefficient of $r = 0.48$ (95% confidence interval: 0.26–0.72). In contrast, Shiina et al. [19], reported no significant correlation between liver parenchymal native T1 and myocardial native T1 values ($p = 0.12$). In our study, liver parenchymal ECV values demonstrated a moderate correlation with myocardial ECV values ($\rho = 0.568$). Similarly, Isaak et al. [20] reported a statistically significant correlation between liver parenchymal and myocardial values in both native T1 mapping ($r = 0.44$) and ECV calculation ($r = 0.43$). These findings suggest that interstitial space expansion in both the myocardium and liver parenchyma occurs in a parallel and correlated manner in patients with reduced ejection fraction, as reflected by both native T1 and ECV values.

Elevated serum GGT activity has been observed from the early stages of HF, which represents the final common pathway of all cardiovascular diseases [21]. In our study, a statistically significant but weak correlation was found between increased liver parenchymal native T1 values and GGT levels in the patient group ($\rho = 0.360$). Bogaert et al. [17] demonstrated that serum GGT levels were significantly correlated with increased liver parenchymal values in both native T1 mapping ($r^2 = 0.34$) and ECV calculations ($r^2 = 0.23$). Considering these findings, we propose that hepatic congestion

resulting from elevated CVP leads to progressive cellular damage. As the extent of congestion increases, a larger number of hepatocytes are affected, leading to elevated GGT levels.

Elevated NT-proBNP levels in HF are associated with increased mortality, morbidity, and recurrent hospital admissions [22]. Furthermore, short-term elevations in NT-proBNP during hospitalization have been shown to predict prolonged hospital stays [23]. In our study, native liver parenchymal T1 values demonstrated a weak but statistically significant positive correlation with NT-proBNP levels ($\rho = 0.324$). Wang et al. [7] also reported a similar correlation in their study. In a prospective study [24], which included 1,075 participants, a positive correlation was observed between elevated liver native T1 values and NT-proBNP levels. This association remained significant in a linear regression model adjusted for age and sex. Based on these, we suggest that as HF progresses, NT-proBNP levels increase in parallel with hepatic congestion, as reflected by elevated liver native T1 values.

Conversely, we did not find a significant correlation between liver parenchymal native T1 values and ALT, AST, or ALP levels in the patient group. In contrast, Mascherbauer et al. [24] reported significant correlations between liver native T1 values and both ALP and AST in their larger cohort. This discrepancy may be explained by our smaller sample size and the predominance of mild HF cases, which might not result in heightened liver enzyme levels.

As part of our study, both intraobserver and interobserver consistency were evaluated. The calculated ICCs and their 95% confidence intervals demonstrated good to excellent agreement in both intraobserver and interobserver assessments, indicating high measurement repeatability. Additionally, the CVs were found to be below 10%, further supporting the reliability of the measurements. These findings suggest that liver parenchymal measurements are highly reproducible and consistent across different observers. Given that the liver is often included within the field of view in routine CMR, this high level of repeatability serves as an important reference point, supporting its potential as a reliable and practical region for evaluation.

This study has several limitations. First, its retrospective and non-invasive nature precluded histopathological validation and differentiation between hepatic edema and fibrosis. Although both edema and fibrosis may increase hepatic T1 values, focal fibrosis or steatosis may also limit the representativeness of the three liver regions sampled on CMR. Second, patients were included based on LVEF <50% regardless of the underlying etiology, resulting in a heterogeneous population that may have introduced confounding, particularly regarding myocardial T1/ECV values and hepatic congestion patterns. Third, the control group was significantly younger than the patient group, despite sex matching, which may have influenced hepatic T1 values. Fourth, right ventricular function and the severity of tricuspid regurgitation were not specifically assessed, limiting evaluation of their potential contribution to hepatic venous congestion. Although patients with known chronic liver disease, including non-alcoholic fatty liver disease, were excluded, other unrecognized hepatic or hemodynamic factors may have affected the measurements. Finally, the single-center, retrospective design may limit the generalizability of our findings. Despite these limitations, the observed differences and consistent associations between hepatic and cardiac parameters support the potential utility of liver T1 mapping and ECV assessment in patients with reduced LVEF.

In conclusion, the findings of our study indicate that CH in patients with reduced LVEF is characterized by prolonged native T1 relaxation times and increased ECV in liver parenchymal mapping—detectable without the need for additional imaging sequences. We propose that liver parenchymal measurements obtained from routinely included CMR mapping sequences are valuable for the early detection of CH, particularly in patients with HF. Further multicenter, prospective studies with larger cohorts are warranted to elucidate pathological changes in the cardiohepatic axis in greater detail using CMR mapping techniques.

Supplementary Information

The online version contains supplementary material available at https://doi.org/10.1186/s43055-026-01849-2.

Additional file 1.

Additional file 2.

Author contributions

Conceptualization: Şahin S, Işıksalan Özbülbül N; Data curation: Şahin S, Yılmaz HÖ, Ilgın C; Formal analysis: Şahin S, Ilgın C, Işıksalan Özbülbül N; Investigation: Şahin S, Yılmaz HÖ, Ilgın C; Methodology: Şahin S, Işıksalan Özbülbül; Supervision: Işıksalan Özbülbül N, Şahin S; Writing—original draft: Şahin S; Writing—review & editing: Şahin S, Işıksalan Özbülbül N.

Funding

The authors received no financial support for the research, authorship, and/or publication of this article.

Data availability

The data generated in this study is available from the corresponding author upon reasonable request.

Declarations

Competing interests

The authors have no financial conflicts of interest.

Ethics approval and consent to participate
This study was approved by the Ankara Bilkent City Hospital No. 2 Scientific and Ethical Review Board for Medical Research (approval No. TABED 2-24-40). The requirement for informed consent was waived because of the secondary analytical study design and the use of anonymized participant data. This study complied with the Declaration of Helsinki (2013) and its amendments.

Consent for publication
Not applicable.

Received: 8 February 2026 Accepted: 24 August 2026
Published online: 01 September 2026

References

1. Hilscher M, Sanchez W (2016) Congestive hepatopathy. Clin Liver Dis 8(3):68–71. https://doi.org/10.1002/cld.573
2. Fortea JI, Puente Á, Cuadrado A et al (2020) Congestive hepatopathy. Int J Mol Sci 21(24):9420. https://doi.org/10.3390/ijms21249420
3. Xanthopoulos A, Starling RC, Kitai T, Triposkiadis F (2019) Heart failure and liver disease. JACC Heart Fail 7(2):87–97. https://doi.org/10.1016/j.jchf.2018.10.007
4. Van Deursen VM, Damman K, Hillege HL, Van Beek AP, Van Veldhuisen DJ, Voors AA (2010) Abnormal liver function in relation to hemodynamic profile in heart failure patients. J Card Fail 16(1):84–90. https://doi.org/10.1016/j.cardfail.2009.08.002
5. Haddadin R, Aboujaoude C, Trad G (2024) Congestive hepatopathy: a review of the literature. Cureus. https://doi.org/10.7759/cureus.58766
6. Carrabba N, Amico MA, Guaricci AI et al (2024) CMR mapping: the 4th-era revolution in cardiac imaging. J Clin Med 13(2):337. https://doi.org/10.3390/jcm13020337
7. Wang J, Diao Y, Xu Y et al (2024) Liver T1 mapping derived from cardiac magnetic resonance imaging: a potential prognostic marker in idiopathic dilated cardiomyopathy. Magn Reson Imaging 60(2):675–685. https://doi.org/10.1002/jmri.29223
8. Huber AT, Razakamanantsoa L, Lamy J et al (2020) Multiparametric differentiation of idiopathic dilated cardiomyopathy with and without congestive heart failure by means of cardiac and hepatic T1-weighted MRI mapping. Am J Roentgenol 215(1):79–86. https://doi.org/10.2214/AJR.19.22009
9. Kazour I, Serai SD, Xanthakos SA, Fleck RJ (2018) Using T1 mapping in cardiovascular magnetic resonance to assess congestive hepatopathy. Abdom Radiol 43(10):2679–2685. https://doi.org/10.1007/s00261-018-1528-x
10. Ostovaneh MR, Ambale-Venkatesh B, Fuji T et al (2018) Association of liver fibrosis with cardiovascular diseases in the general population: the Multi-Ethnic Study of Atherosclerosis (MESA). Circ Cardiovasc Imaging 11(3):e007241. https://doi.org/10.1161/CIRCIMAGING.117.007241
11. McDonagh TA, Metra M, Adamo M, et al. (2021) ESC Guidelines for the diagnosis and treatment of acute and chronic heart failure: Developed by the Task Force for the diagnosis and treatment of acute and chronic heart failure of the European Society of Cardiology (ESC). With the special contribution of the Heart Failure Association (HFA) of the ESC. Euro J of Heart Fail. 2022;24(1):4-131.https://doi.org/10.1002/ejhf.2333
12. Gottbrecht M, Kramer CM, Salerno M (2019) Native T1 and extracellular volume measurements by cardiac MRI in healthy adults: a meta-analysis. Radiology 290(2):317–326. https://doi.org/10.1148/radiol.2018180226
13. Yucel-Finn A (2024) Cardiac. In: Balasubramaniam R, ed. *Chapman & Nakielny's Guide to Radiological Procedures*. 239–262. https://doi.org/10.1016/B978-0-323-93363-6.00009-7
14. Cassinotto C, Feldis M, Vergniol J et al (2015) MR relaxometry in chronic liver diseases: comparison of T1 mapping, T2 mapping, and diffusion-weighted imaging for assessing cirrhosis diagnosis and severity. Eur J Radiol 84(8):1459–1465. https://doi.org/10.1016/j.ejrad.2015.05.019
15. Banerjee R, Pavlides M, Tunnicliffe EM et al (2014) Multiparametric magnetic resonance for the non-invasive diagnosis of liver disease. J Hepatol 60(1):69–77. https://doi.org/10.1016/j.jhep.2013.09.002
16. De Lange C, Reichert MJE, Pagano JJ et al (2019) Increased extracellular volume in the liver of pediatric Fontan patients. J Cardiovasc Magn Reson 21(1):39. https://doi.org/10.1186/s12968-019-0545-4
17. Bogaert J, Symons R, Rafouli-Stergiou P, Droogné W, Dresselaers T, Masci PG (2021) Assessment of right-sided heart failure in patients with dilated cardiomyopathy using magnetic resonance relaxometry of the liver. Am J Cardiol 149:103–111. https://doi.org/10.1016/j.amjcard.2021.03.012
18. Beigh MVR, Pajunen KBE, Pagano JJ et al (2022) T1 mapping of the myocardium and liver in the single ventricle population. Pediatr Radiol 53(6):1092–1099. https://doi.org/10.1007/s00247-022-05560-y
19. Shiina Y, Inai K, Ohashi R, Nagao M (2021) Potential of liver T_1 mapping for the detection of Fontan-associated liver disease in adults. MRMS 20(3):295–302. https://doi.org/10.2463/mrms.mp.2020-0063
20. Isaak A, Praktiknjo M, Jansen C et al (2020) Myocardial fibrosis and inflammation in liver cirrhosis: MRI study of the liver-heart axis. Radiology 297(1):51–61. https://doi.org/10.1148/radiol.2020201057
21. Jiang S, Jiang D, Tao Y (2013) Role of gamma-glutamyltransferase in cardiovascular diseases. Exp Clin Cardiol 18(1):53–56
22. Novack ML, Zubair M (2024) Natriuretic peptide B type test. StatPearls. StatPearls Publishing
23. Savarese G, Musella F, D'Amore C et al (2014) Changes of natriuretic peptides predict hospital admissions in patients with chronic heart failure. JACC Heart Fail 2(2):148–158. https://doi.org/10.1016/j.jchf.2013.11.007
24. Mascherbauer K, Donà C, Koschutnik M et al (2022) Hepatic T1-time predicts cardiovascular risk in all-comers referred for cardiovascular magnetic resonance: A Post-Hoc analysis. Circ Cardiovasc Imag 15:10. https://doi.org/10.1161/CIRCIMAGING.122.014716

Publisher's Note

Springer Nature remains neutral with regard to jurisdictional claims in published maps and institutional affiliations.